For Duke Conference on Hyperon Resonances, Durham, North Carolina, April 24-25, 1970

UCRL-19765
Preprint

c. 2

Λ (1520) REVISITED

Robert D. Tripp

May 1970

AEC Contract No. W-7405-eng-48

LAWRENCE RADIATION LABORATORY
UNIVERSITY of CALIFORNIA BERKELEY

UCRL-19765

DISCLAIMER

Λ (1520) REVISITED

Robert D. Tripp

Lawrence Radiation Laboratory

Berkeley, California 94720

K^--proton interactions in the region below 500 MeV/c have been under investigation by bubble chambers for many years. The general behavior of the dominant S-wave amplitudes in both I = 0 and 1 and resonant D_{03} amplitude now seem fairly well understood. However, considerable uncertainty remains concerning the smaller P- and D-wave amplitudes. Large scale bubble chamber experiments now in their final stages of analysis should soon clarify the situation.

Figure 1 is a compilation of a decade of K^-p path length from 0 to 500 MeV/c. The seven experiments[1-7] displayed are described in the figure caption. Notice that the ordinate is logarithmic so that the K-65 experiment for example has about 100 times the path length of the earlier WFT experiment in the region of Λ(1520). In this report I shall review the experimental situation in the vicinity of Λ(1520), the region covered by the old experiment of Watson, Ferro-Luzzi, and Tripp[4] (WFT), and the recent experiments of Brookhaven, Massachusetts, and Yale[5] (BMY) and of the Berkeley group[6] (K-65).

Following the discovery and establishment of the quantum numbers of Λ(1520) by WFT, this resonance was seen over the years in a number of production experiments.[8] These production experiments gave a branching fraction for Λ(1520) into $\bar{K}N$ of about 0.45 whereas the elasticity found by WFT was only 0.30. One would normally be inclined to favor the formation experiment because of the intrinsically more detailed analysis to which the data are amenable. However, in the production experiments Λ(1520) was often produced comparatively free from background, and it is difficult to fault their straightforward results. K-65 now finds that an elasticity of 0.45

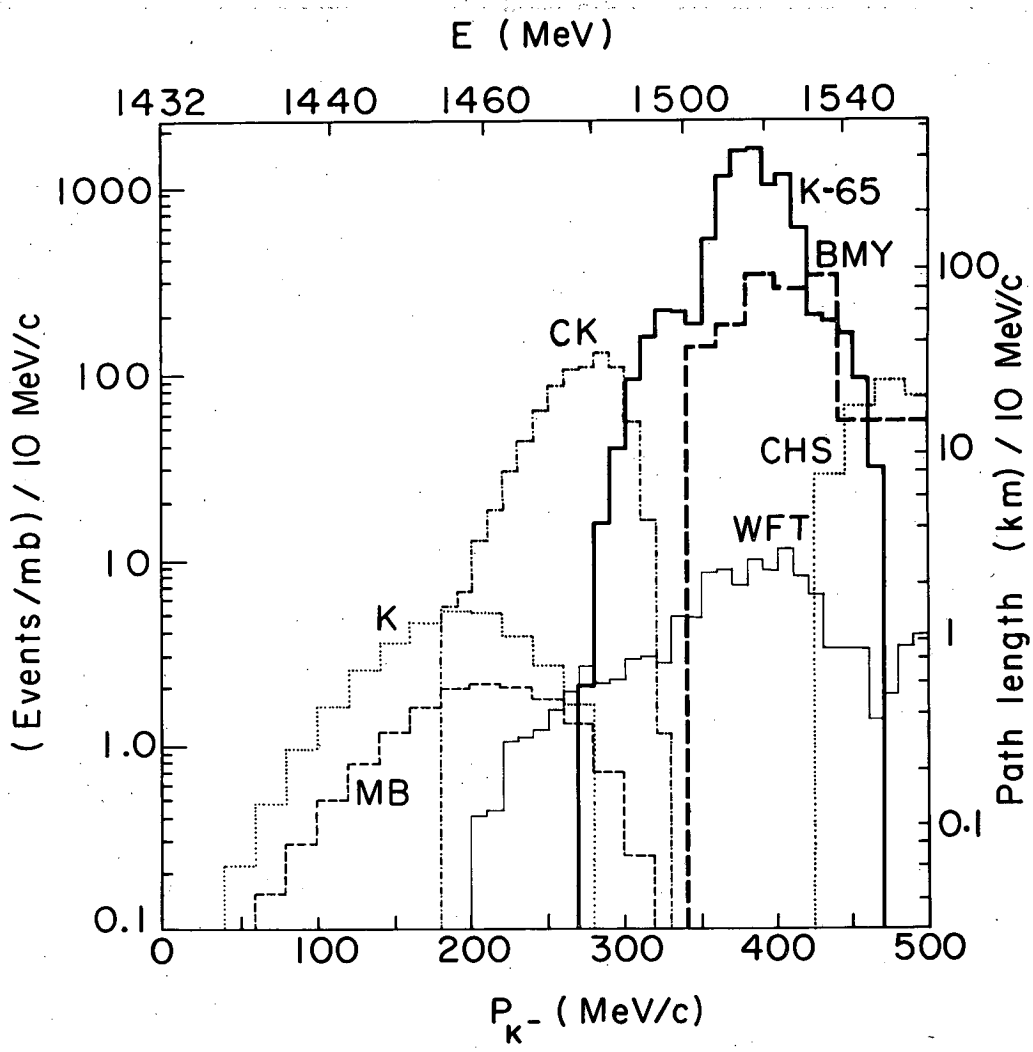

FIG. 1. Path lengths for the seven major hydrogen bubble chamber experiments on K^-p interactions from 0 to 500 MeV/c. The abbreviations are as follows: K(Kim[1]), MB(Maryland-Berkeley[2]), CK (Chan and Kadyk[3]), WFT(Watson, Ferro-Luzzi, and Tripp[4]), BMY (Brookhaven, Massachusetts, and Yale[5]), K-65(unpublished Berkeley experiment[6]), and CHS(CERN, Heidelberg, and Saclay[7]). The BMY path length shown corresponds only to that part which has been analyzed for certain strong interactions; their total path length in the region of $\Lambda(1520)$ is comparable with K-65.

is indeed correct and it is instructive to see how the low elasticity found by WFT came about.

Figure 2 shows the angular distribution of K^-p elastic scattering in the vicinity of $\Lambda(1520)$ to have a very strong $\cos^2\theta$ dependence in the data of K-65. The corresponding data of WFT appear in Fig. 3,

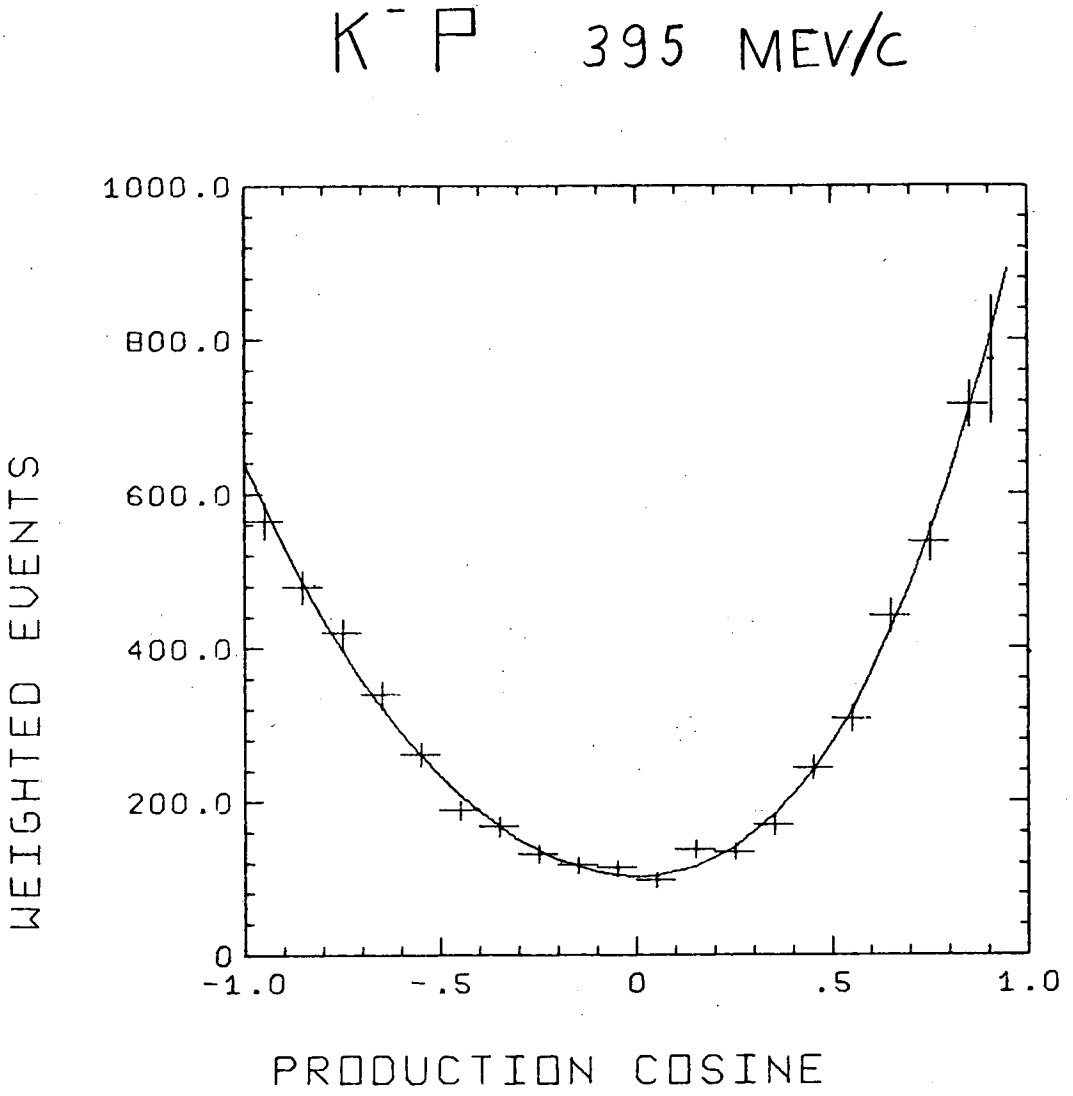

FIG. 2. K^-p elastic angular distribution in the momentum interval 390 to 400 MeV/c as measured by K-65.

where at 390 MeV/c the $\cos^2\theta$ term is seen to be less pronounced and to rapidly disappear at momenta above and below the resonance. Fig. 4 shows this effect more quantitatively. Here the ratio A_2/A_0 in the Legendre polynomial expansion of the elastic angular distribution (which is a measure of the amount of $\cos^2\theta$) is exhibited as a function of the K^- laboratory momentum for both K-65 and WFT. There is a clear disagreement in the vicinity of the resonance. This we now understand to be mainly a result of the poor momentum resolution in the latter experiment. The experimentally measured momentum resolution of WFT is shown in Fig. 5. The peculiar double-peaked structure is due to the fact that the forward and backward scatters result in a stopping particle whose momentum is well measured by range, whereas the group of events with a resolution of

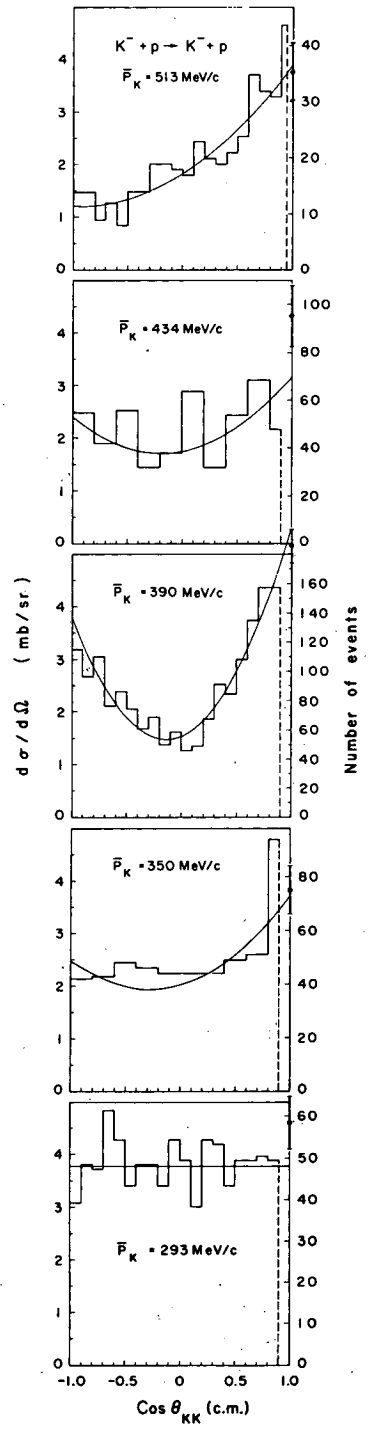

FIG. 3. K^-p elastic angular distributions in five different momentum regions as measured by WFT.

about 12 MeV/c are those particles scattered near 90 deg, where both particles leave the chamber. However, not even a resolution function as large as 12 MeV/c when folded into the new data is sufficient to reconcile the two experiments; at least 15 MeV/c is required. The poor momentum resolution of WFT compared to K-65 arises from three causes:

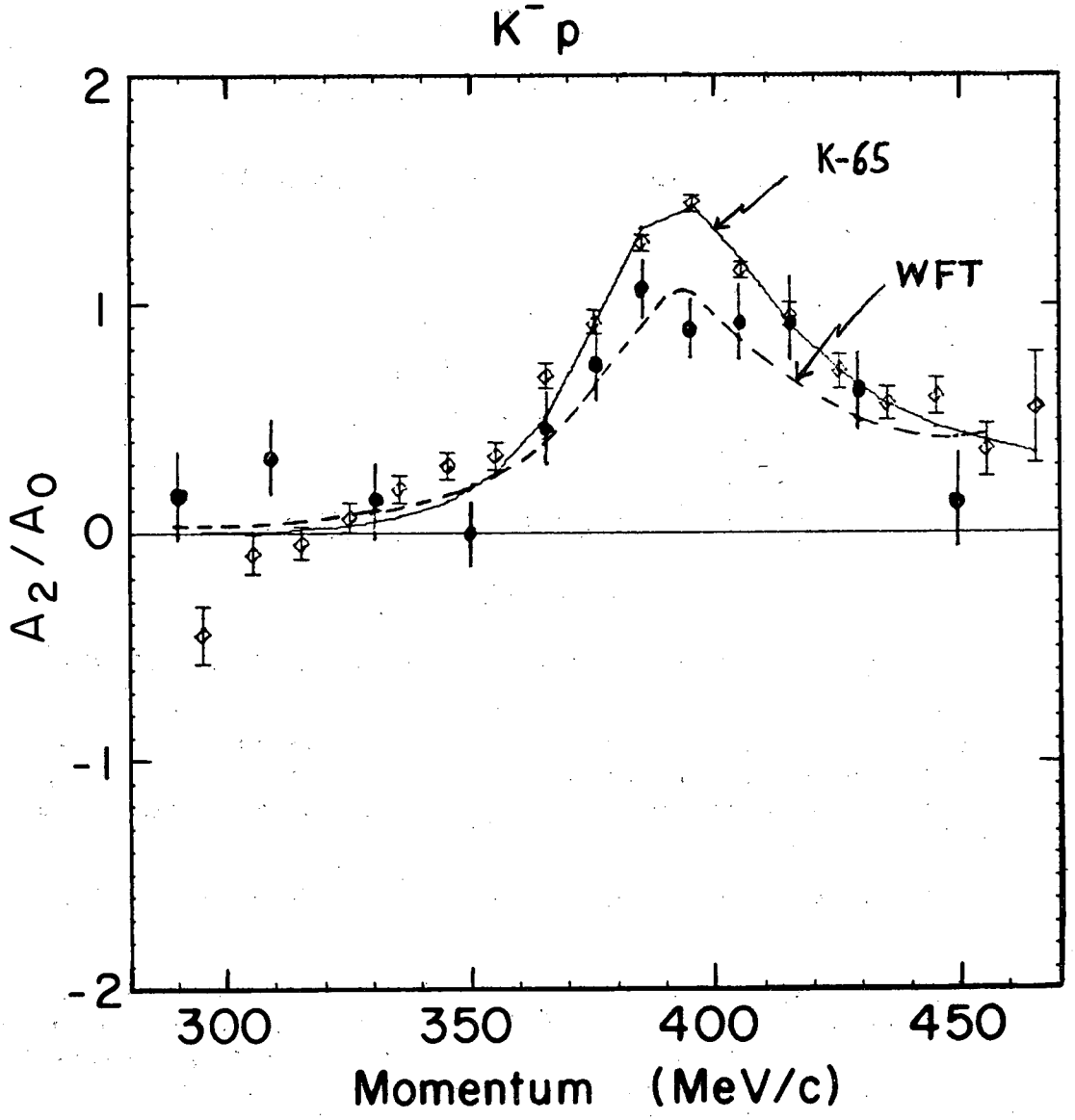

FIG. 4. The ratio A_2/A_0 in the Legendre polynomial expansion of the K^-p angular distribution vs momentum. Open diamonds are data from K-65; solid circles are data from WFT. The solid line and dashed lines are multichannel scattering length fits to the corresponding data.

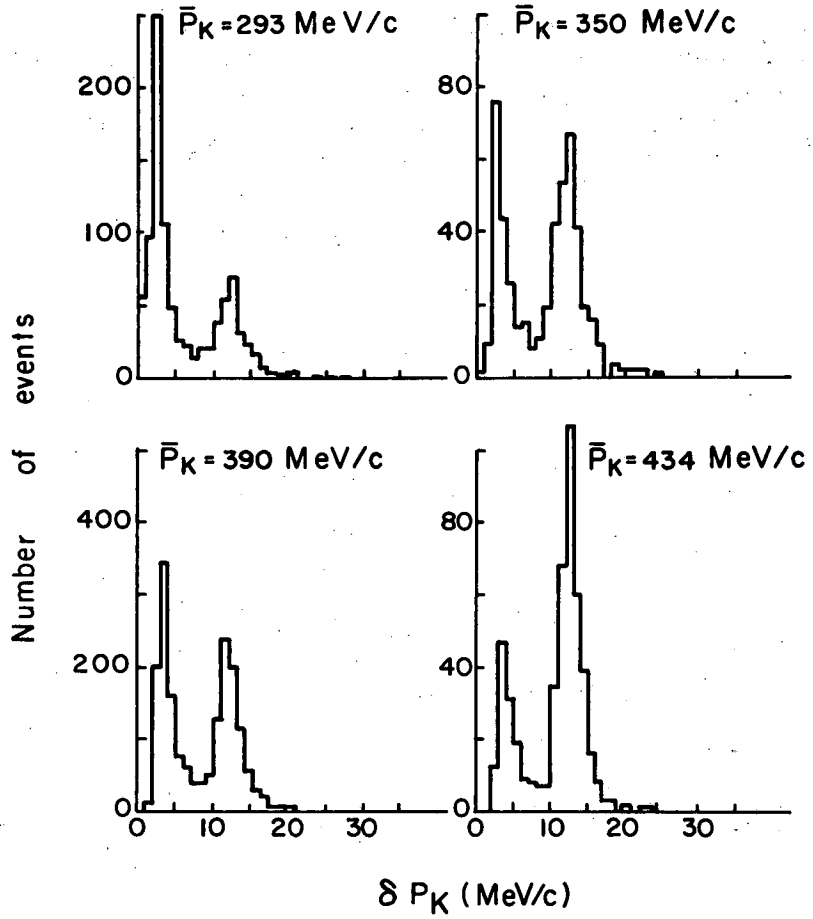

FIG. 5. Experimentally measured momentum resolution of WFT.

(1) The beam was degraded from 760 MeV/c so that the momentum uncertainty on an incoming track was about 30 MeV/c, whereas in K-65 degraders were not used and the momentum spread was less than 5 MeV/c.

(2) The chamber magnetic field was about 11 kG vs 18.7 kG for K-65.

(3) The 15-inch chamber used by WFT had perhaps the world's worst turbulence and gave χ^2 distributions for fitted events that were considerably too large, leading to error assignments that were underestimated by about 20%. The momentum scale in Fig. 5 should therefore be increased by this factor.

Because the K^-p elastic cross section is so much larger than reactions with better momentum resolution, such as $K^-p \rightarrow \bar{K}^0 n$, it dominated in the χ^2 fitting of the coupled-channel analysis. Hence the solution of WFT followed the trend of elastic data whereas it

did not reproduce the bump observed in the charge-exchange cross section, as can be seen in Fig. 6. Here an elasticity 50% greater would increase the resonance bump by 2.25, resulting in a better fit.

This dramatizes some of the problems of a detailed high-statistics analysis, serving as an apology for why, after a number of years, the newer experiments have not as yet produced final results. Later I shall return to a discussion of the branching fractions for $\Lambda(1520)$ as now measured in K-65.

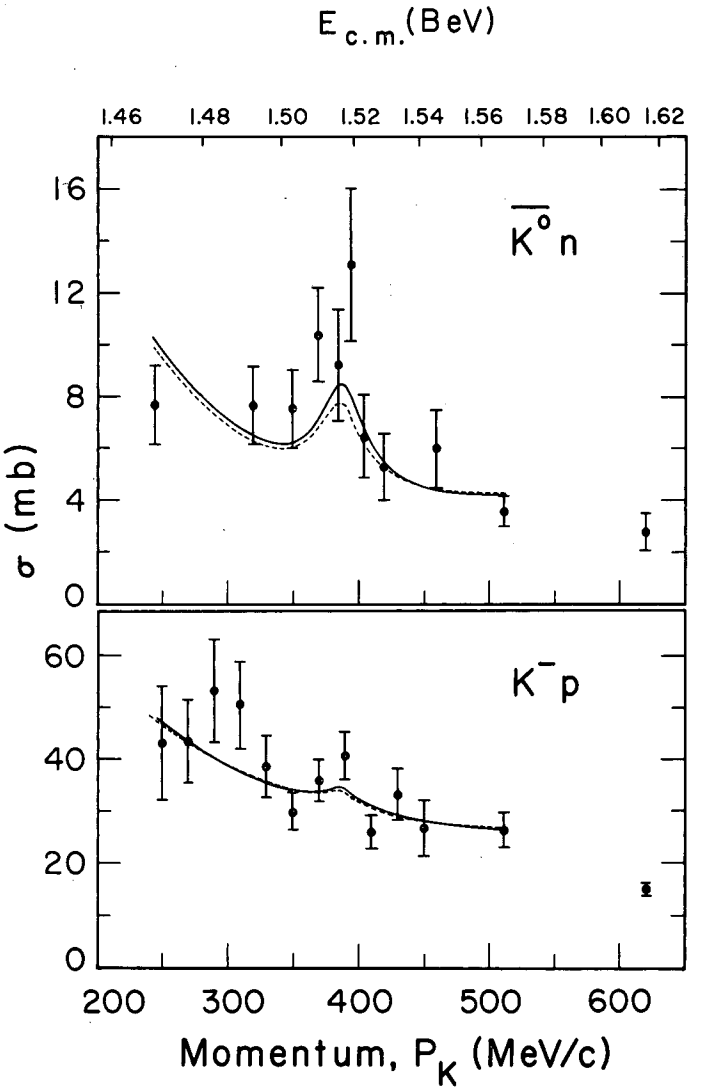

FIG. 6. Cross sections for K^-p charge exchange and elastic scattering as a function of momentum as measured by WFT. The solid lines represent the best fit to all the data in the coupled-channel analysis of WFT.

The BMY group has recently submitted for publication[5] a coupled-channel partial-wave analysis of the K^-p system from 350 to 430 MeV/c. Since they have analyzed only the "0 prong V^0 topology" (i.e. $\bar{K}^0n$, $\Lambda\pi^0$, and $\Sigma^0\pi^0$), they have included in their analysis, data for other channels as reported by WFT as well as some published data on Σ polarization from K-65.[6] That they have residual experimental problems is evident in Fig. 7 where their charge-exchange coefficients are shown as a function of momentum. Considerable disagreement between two runs at different momenta is apparent in the overlap region at 390 MeV/c. Their best-fit solution predicts only a very small bump in the charge-exchange cross section. This, as in the analysis of WFT, is probably a result of poor momentum resolution. Thus they report an elasticity for $\Lambda(1520)$ of only 0.26, which is even lower than that of WFT, while the resonant width comes out to be 26 MeV, some 50% too large. Figure 8 summarizes their elastic partial-wave amplitudes for the S and P waves parametrized either with effective ranges or constant K matrices. Also shown are the amplitudes of Kim[9] and Martin and Sakitt[10] for the S waves.

Turning now to a discussion of the preliminary data of K-65,[6] covering the momentum range from 280 to 470 MeV/c, Table I lists the seven channels involved in the coupled-channel analysis with the number of measured events in each channel. Apart from the elastic scatters, nearly all events on the film were measured so that these represent essentially the number of events for each channel within the fiducial volume. Only about 10% of the two prongs (elastic scatters) were measured in the momentum region from 350 to 420 MeV/c where, as can be seen in Fig. 1, some 83% of the K-65 path length is contained. From 280 to 350 MeV/c (10% of the path length) and from 420 to 470 MeV/c (7% of the path length), nearly all the elastic scatters were measured. For the entire experiment the total number of measurements was about 1/2 million. The immense job of analyzing all this data is in the able hands of our graduate student Terry Mast and research associate Roger Bangerter.

We have used two different energy-dependent expressions for the nonresonant partial-wave amplitudes: 1) a constant scattering length parametrization in a manner essentially identical to that of WFT, and 2) parametrization of the S_{01}, S_{11}, and P_{13} amplitudes by means of the Ross and Shaw[11] effective range. The latter, with a number of extra parameters, produces only a slightly improved χ^2 despite the fact that, barring anomalies, it should give a more exact description of the true energy dependence of these amplitudes. This illustrates the point that when fitting over a limited energy region, extraction of the energy dependence of the amplitudes is extremely difficult. However, once we incorporate into the analysis the published lower-energy data and perhaps some at higher energy from other experiments, meaningful effective range parameters probably can be deduced.

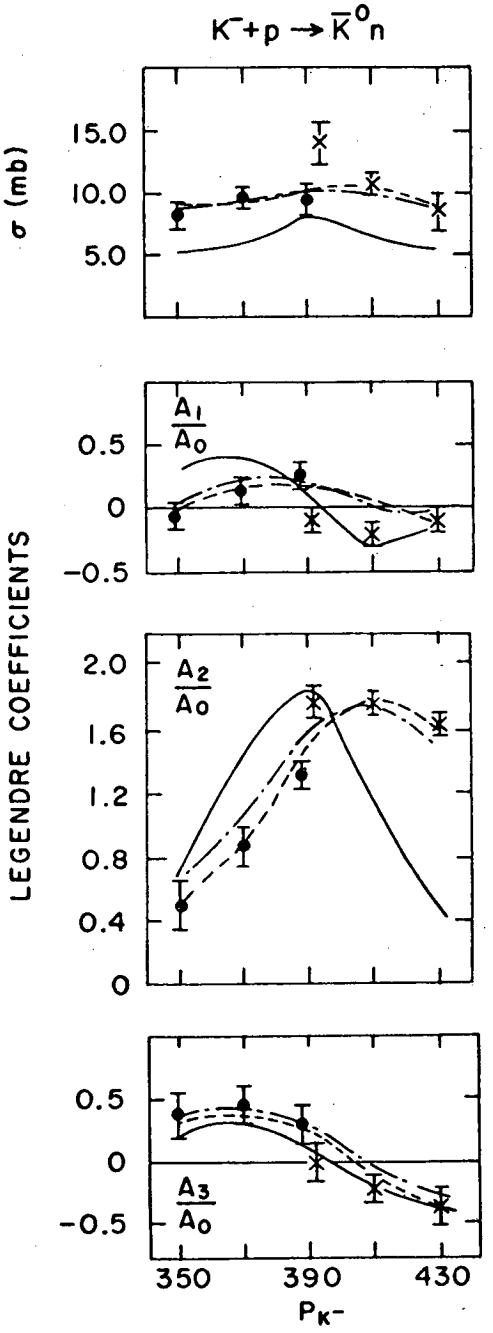

FIG. 7. Charge-exchange angular distribution coefficients from the BMY experiment as a function of momentum. Solid circles and crosses correspond to two different momentum settings. The solid curves are predictions from J. Kim[9] based on older data; the other curves are K matrix fits of BMY.

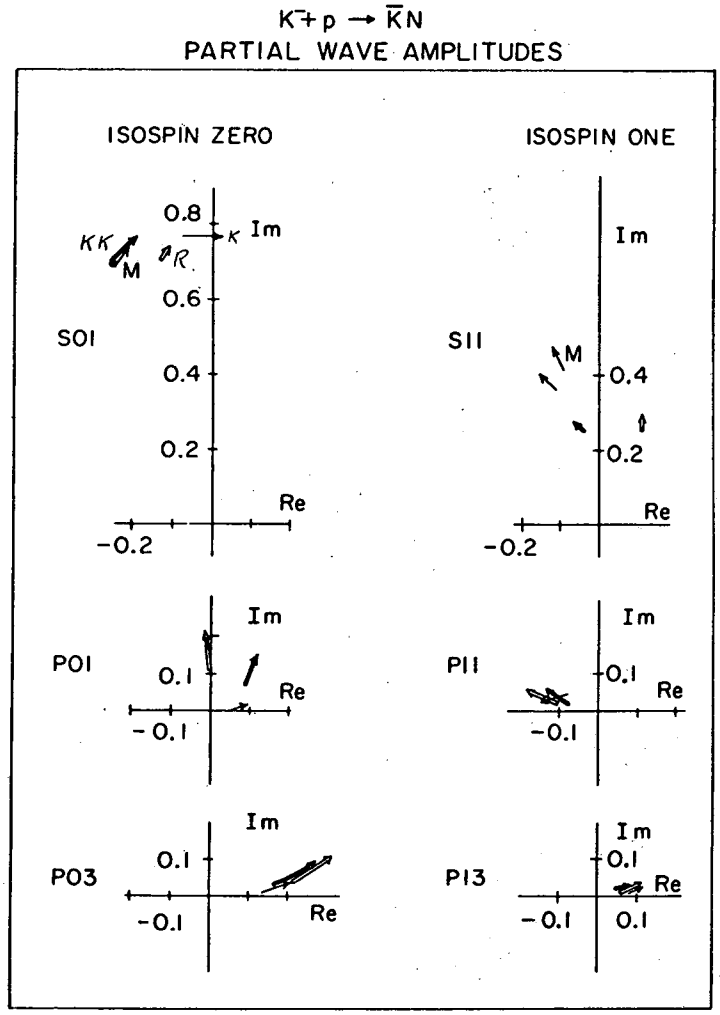

FIG. 8. Elastic partial-wave amplitudes of BMY. The beginning of the arrow is at 350 MeV/c and the tip at 430 MeV/c. Shown are the constant K-matrix (KK) and effective-range (R) analysis of BMY, as well as the solution of Kim (K) and Martin and Sakitt (M) for the S wave.

Table I summarizes the χ^2 obtained from the constant scattering length fit broken down according to channel and according to whether it arises from the partial cross section, differential cross-section polynomial coefficients, or polarization polynomial coefficients. The polarization coefficients fit best; this is reasonable since they should be least affected by the expected biases. The cross sections fit least well, owing mainly to continuing problems associated with the different momentum resolution of the tau decays from which the path length is determined, compared to that from various other topologies. The elastic scatters and $Y^0\pi^0$ channels are still in quite preliminary form, while for the other channels we

Table I. The ratio of χ^2 to expected χ^2 according to channel and type of measurement for K-65.

		$\chi^2/\langle\chi^2\rangle$		
Channel	Measured events	σ	A_n/A_0	B_n/A_0
K^-p	46,000		2.23	
$\bar{K}^0N$	30,000	1.34	1.80	
$\Sigma^+\pi^-$	85,000	1.85	1.61	0.87
$\Sigma^-\pi^+$	61,000	1.74	0.98	1.25
$\Sigma^0\pi^0$	40,000	1.89	2.71	1.27
$\Lambda\pi^0$		2.18	1.09	0.99
$\Lambda\pi^+\pi^-$	10,000	1.77		
Total	272,000	1.86	1.71	1.07

Overall $\chi^2/\langle\chi^2\rangle = 1.45 \pm 0.05$

do not anticipate substantial changes in the final data. The overall ratio of χ^2 to expected χ^2 is 1.45 ± 0.05, so in a chi-squared sense the fit is poor. However, the general trend of the data and nearly all structure is fit rather well. In Fig. 9 the ratio $\chi^2/\langle\chi^2\rangle$ is plotted as a function of momentum for this solution. If the assumed momentum dependence of the amplitudes is responsible for the high χ^2, then, since most of the path length is from 350 to 420 MeV/c, one would expect that this region would fix the amplitudes and that both above and below this region the χ^2 would rise. Such a behavior is not observed. Conversely, systematic effects will show up most visibly in the region containing most data. Since χ^2 is not enhanced here, this cannot be the primary reason for high χ^2. Perhaps a combination of both effects gives rise to the momentum independence observed in Fig. 9.

In order to explore the possibility of unexpected structure in the momentum dependence of the amplitudes, we have broken the data into three momentum intervals centered at 325, 395, and 425 MeV/c. All amplitudes were free to vary in each interval [except for a fixed mass and width of $\Lambda(1520)$]. The χ^2 did not improve, suggesting again that systematic effects rather than improper momentum dependence is the major source of high χ^2. Figures 10, 11, and 12 show the Argand plots for these amplitudes. Figures 13 and 14 show the corresponding $\bar{K}N$ S-wave amplitudes and S- and P-wave amplitudes for other low-energy experiments as compiled by Levi-Setti for the 1969 Lund Conference.[8] The clockwise behavior of the

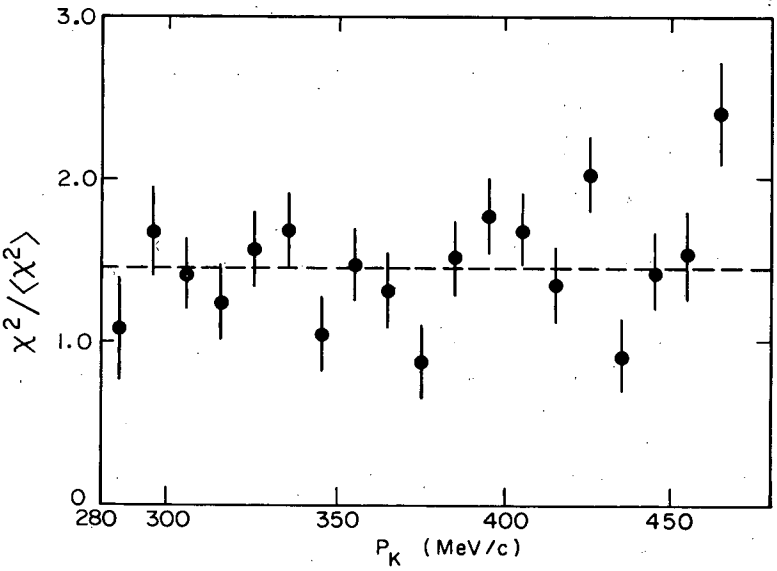

FIG. 9. The ratio of χ^2 to expected χ^2 as a function of momentum for a solution of an energy-dependent coupled-channel analysis of K^-p reactions in the K-65 experiment.

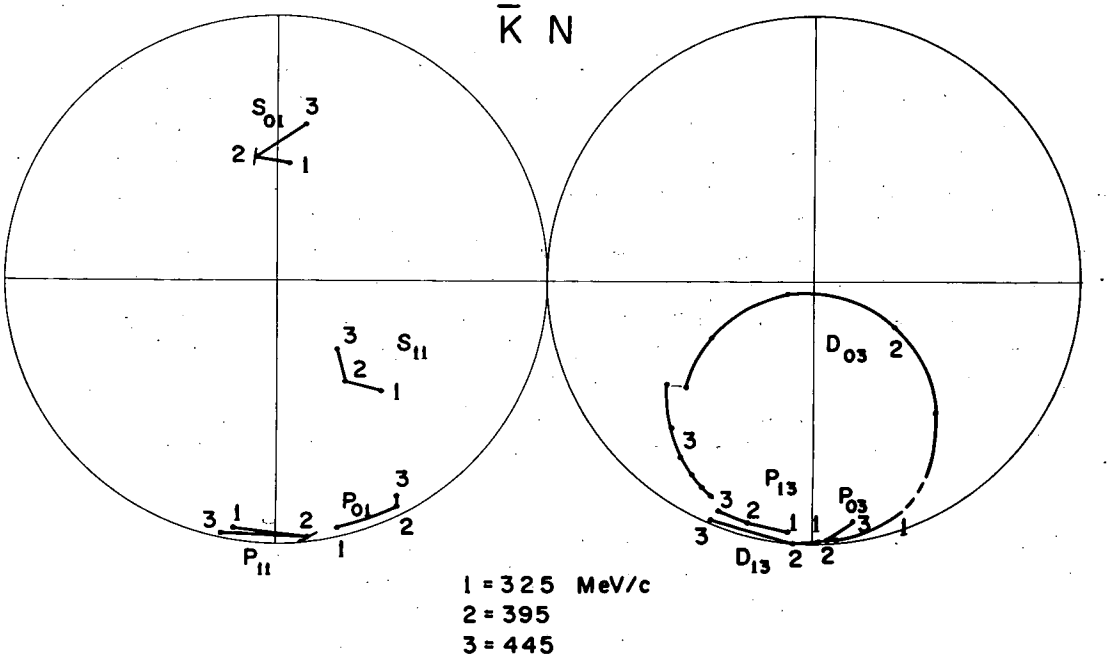

FIG. 10. $\bar{K}N$ amplitudes from the K-65 experiment with data broken into three momentum intervals centered at (1) 325 MeV/c, (2) 395 MeV/c, and (3) 425 MeV/c. The coupled-channel analysis was done in the constant scattering-length approximation except for the resonant D_{03} amplitude. Typical variations over fitted momentum intervals are indicated by several thin lines.

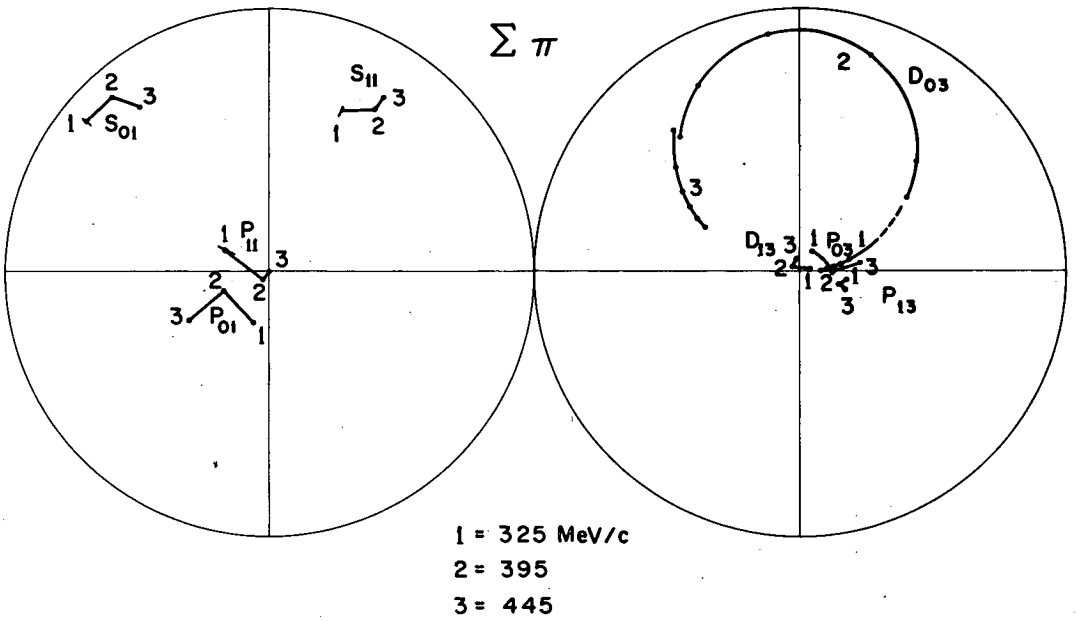

FIG. 11. Same as Fig. 10, but for the $K^- p \rightarrow \Sigma\pi$ amplitudes.

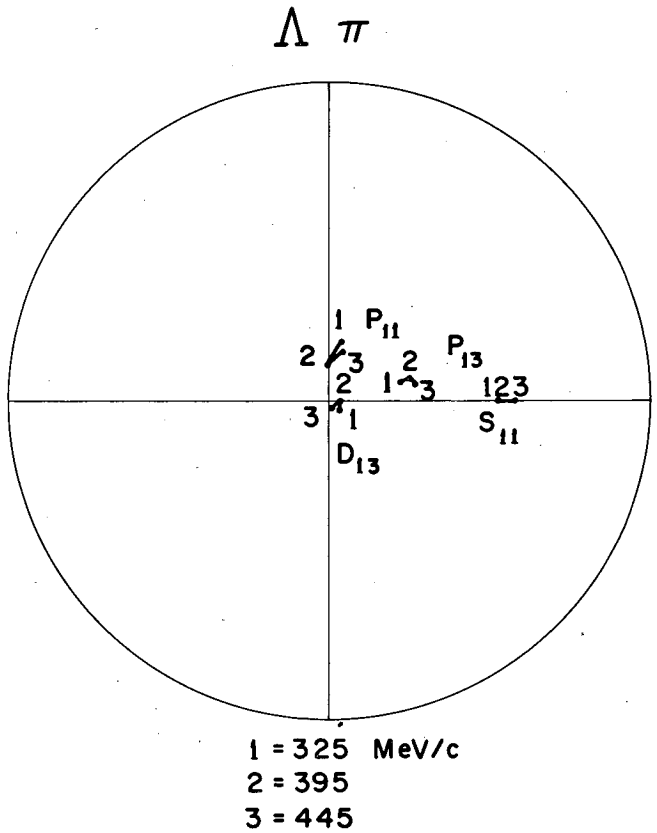

FIG. 12. Same as Fig. 10, but for the $K^- p \rightarrow \Lambda\pi$ amplitudes.

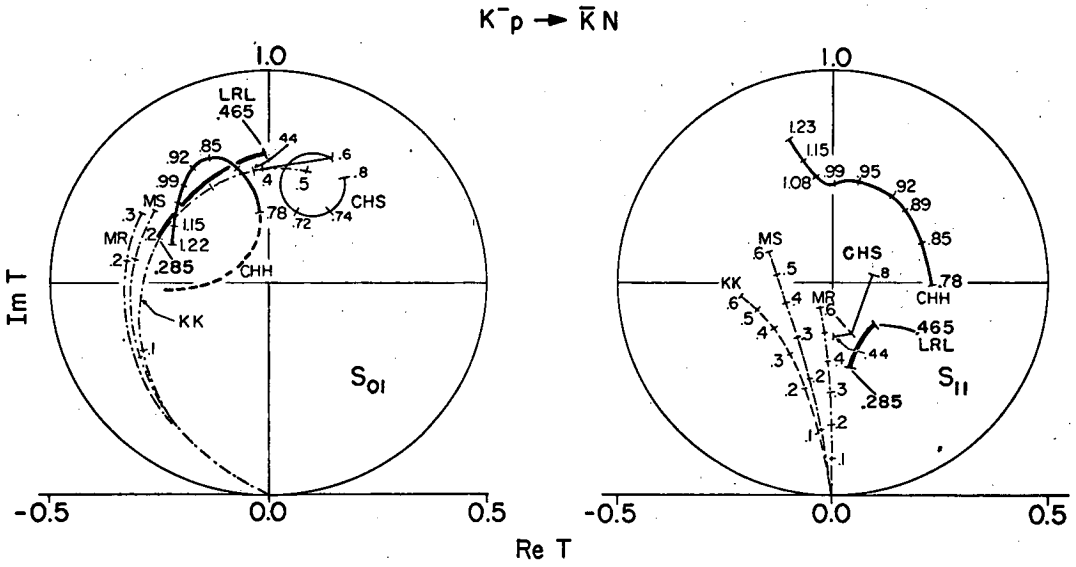

FIG. 13. A compilation[8] of the low energy $K^-p \rightarrow \Sigma\pi$ amplitudes.

$\bar{K}N$ S_{01} amplitude indicated by the low-energy K-matrix solutions in Fig. 13 is not strongly suggested by our data in Fig. 10, but probably there is sufficient uncertainty in our lowest-energy point to accommodate such a behavior. In the $\Sigma\pi$ channel the agreement is better. Perhaps the only anomalous structure suggested by Fig. 10 [apart from the D_{03} amplitude for $\Lambda(1520)$ which is parametrized as a resonance] is some possible structure in the $\bar{K}N$ P_{11} state. However, it must be emphasized that both the data and analysis are preliminary.

New branching fractions for $\Lambda(1520)$ were reported by K-65 at the Lund Conference. We have updated them with some minor changes for this conference with the percentages listed in Fig. 15. The numbers are still not final, but they should not change outside of the indicated statistical uncertainty. The figure also shows some other mass-dependent effects associated with $\Lambda(1520)$ branching fractions. Starting on the left are the branching fractions predicted for a pure SU_3 singlet. Next the $\bar{K}N$-$\Sigma\pi$ mass difference splits them as indicated; however, the experimental shift is in the opposite sense as shown in the middle column. This can be reconciled by introducing a mixing angle of 18 deg between the $3/2^-$ singlet and octet, thereby also greatly improving the agreement of the octet $\Lambda(1690)$ decay rates with decay rates for other members of that octet. We have further introduced different centrifugal barriers for decays into different charge states. This reduced χ^2 slightly (by about 1%) and gave the branching fractions depicted in the next column. Finally, in order to see if the electromagnetic mass splittings (which are comparable to the half-width of the resonance) could lead to further violations of isospin than those embodied in the centrifugal barrier

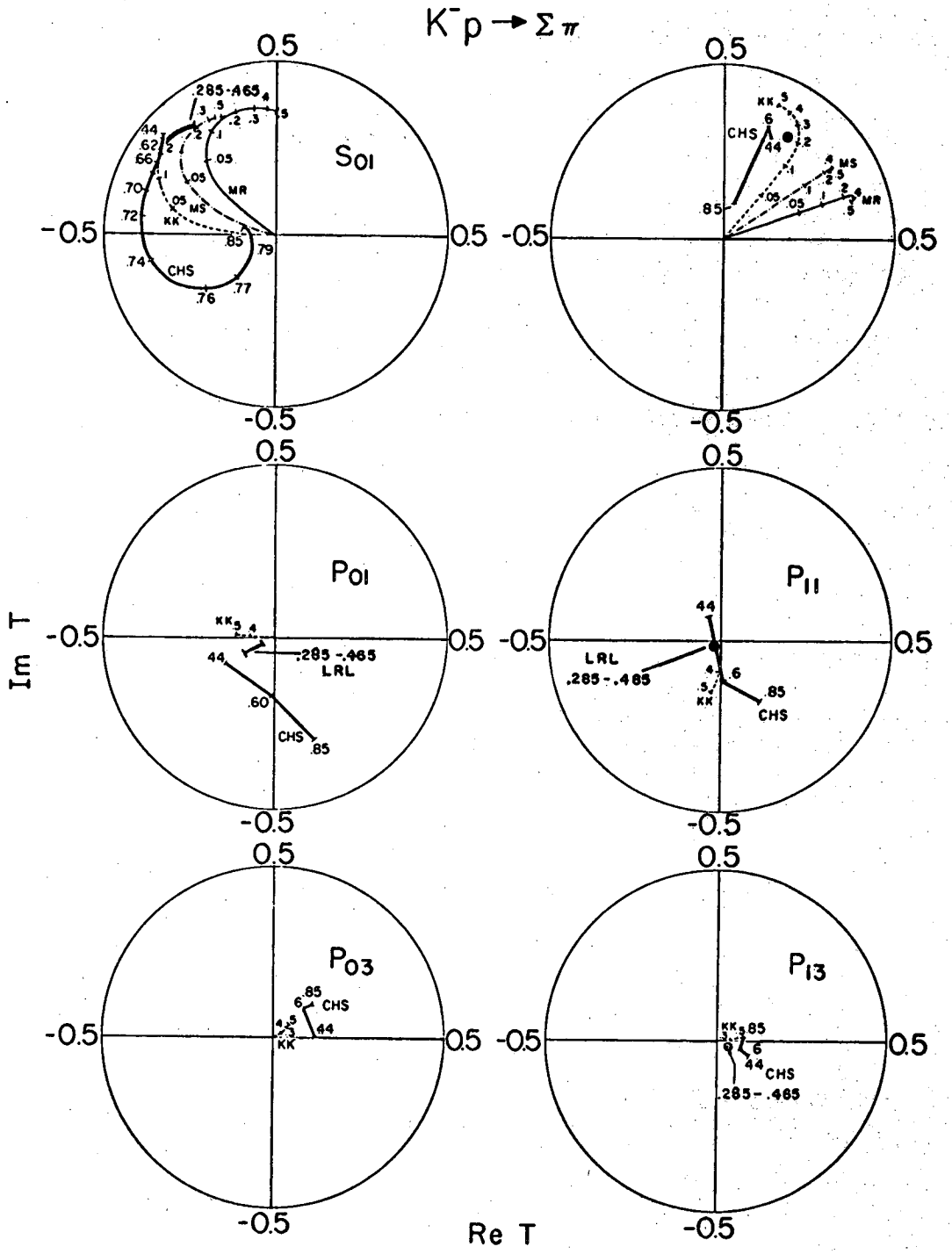

FIG. 14. A compilation[8] of the low energy $K^-p \to \Sigma\pi$ amplitudes.

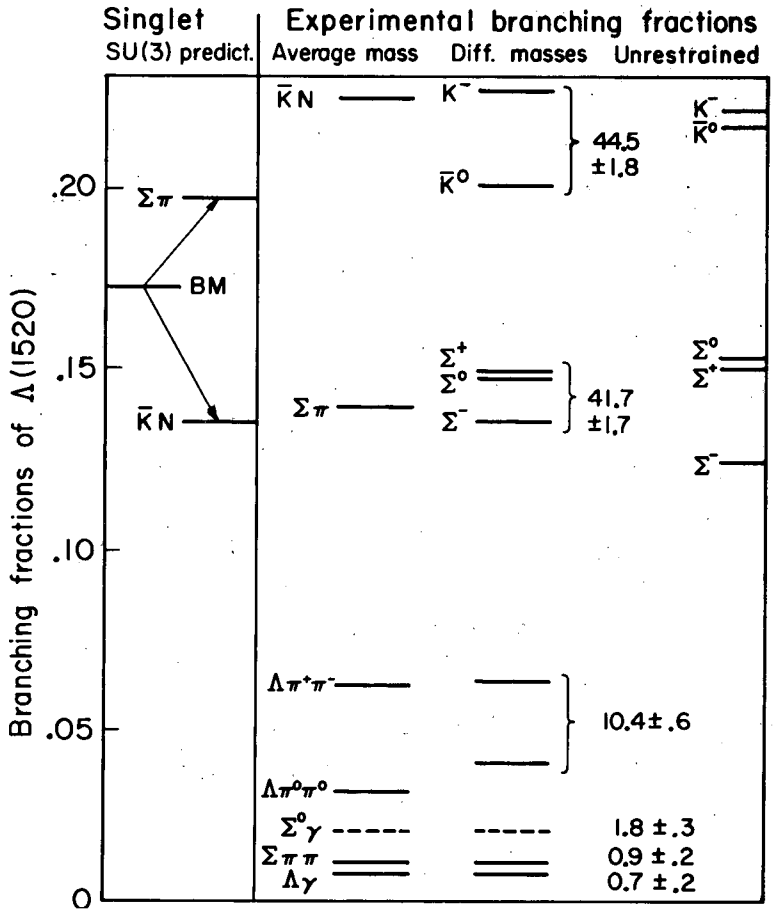

FIG. 15. Branching fractions for $\Lambda(1520)$.

corrections, we have left all $\bar{K}N$ and $\Sigma\pi$ branching fractions unrestrained, thereby introducing three new parameters into the analysis. The χ^2 again lowered by only about 1% and gave the branching fractions illustrated in the last column. They are sufficiently close to those of the previous column that within errors we have no indication of isospin violation in the decay of $\Lambda(1520)$.

As a further test of isospin conservation we have studied the charge-independence triangle formed by the $\Sigma^+\pi^-$, $\Sigma^-\pi^+$, $\Sigma^0\pi^0$ reaction amplitudes at various momenta and angles. Specifically, charge independence requires that $\vec{T}_+ + \vec{T}_- + 2\vec{T}_0 = 0$, where T represents the reaction amplitude at a given angle and the subscript indicates the Σ charge state. Violation of charge independence is indicated by nonclosure of the triange, which can be expressed by the condition that the area of the triangle be ≤ 0. This leads to the requirement for charge independence

$$2\sigma_+\sigma_- + 8\sigma_+\sigma_0 + 8\sigma_-\sigma_0 - \sigma_+^2 - \sigma_-^2 - 16\sigma_0^2 \geq 0,$$

where σ denote the differential cross section in the charge state indicated by the subscript. A preliminary test at 20 angles and 17 momenta using quite primitive $\Sigma^0\pi^0$ data yielded no statistically significant indication of charge-independence violation at any of the 340 points. Final data will be subjected to this test in the near future. Since the reaction amplitude at any angle is composed of many partial waves, this is a more gross test of charge independence, although less model-dependent than the one specific to $\Lambda(1520)$.

Future plans for the K-65 experiment call for the introduction of the full correlation matrix into the coupled-channel analysis of the polynomial coefficients. This will certainly give an improved solution and may reduce the overall χ^2. It is also planned to introduce the effective range matrix parametrization into all partial waves. Although this will bring in many new parameters, it is hoped that an improved χ^2 will result. Finally, there are some hints of structure in the data that we cannot accommodate at the present time. The most prominent is shown in the A_1/A_0 coefficient for K^-p elastic scattering in the vicinity of 425 MeV/c as seen in Fig. 16. If such structure persists in the final data it is difficult to see how it can be accommodated in the present parametrization with only one resonant amplitude.

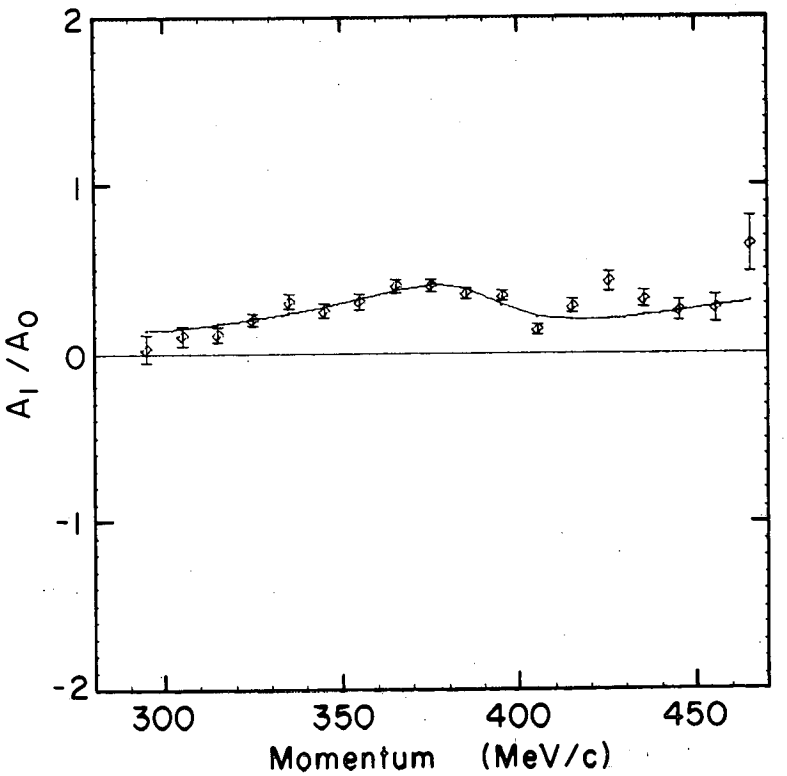

FIG. 16. The A_1/A_0 coefficient vs momentum for K^-p elastic scattering from K-65.

REFERENCES

1. J. K. Kim, Phys. Rev. Letters 14, 29 (1965).
2. M. Sakitt et al., Phys. Rev. 139, B719 (1965).
3. J. Chan and J. Kadyk, private communication of an unpublished Berkeley experiment.
4. M. B. Watson, M. Ferro-Luzzi, and R. D. Tripp, Phys. Rev. 131, 2248 (1963).
5. D. Berley et al., Phys. Rev. (to be published).
6. Some of the $\Sigma^{\pm}$ data appears in R. Bangerter et al., Phys. Rev. Letters 17, 495 (1966) and R. Bangerter, Lawrence Radiation Laboratory Report UCRL-19244, July 1969.
7. R. Armenteros et al., CERN/D. Ph. II/Phys 70-7; submitted to Nuclear Physics B.
8. R. Levi-Setti, in Proceedings of the Lund International Conference on Elementary Particles, 1969 (Berlingska Boxboktryckeriet, Lund, Sweden, 1969).

TECHNICAL INFORMATION DIVISION
LAWRENCE RADIATION LABORATORY
UNIVERSITY OF CALIFORNIA
BERKELEY, CALIFORNIA 94720